Investigating the stress distribution of single walled carbon nanotubes embedded in polyimide nanocomposites

Shi-Hua Tzeng and Jia-Lin Tsai

Journal of Reinforced Plastics and Composites 2011 30: 922 originally published online 14 September 2011
DOI: 10.1177/0731684411421637

Article

JOURNAL OF REINFORCED PLASTICS & COMPOSITES

Journal of Reinforced Plastics and Composites
30(11) 922–931

DOI: 10.1177/0731684411421637
jrp.sagepub.com
SAGE

Investigating the stress distribution of single walled carbon nanotubes embedded in polyimide nanocomposites

Shi-Hua Tzeng and Jia-Lin Tsai

Abstract

The stress distribution of CNTs embedded within polyimide matrix subjected to applied loading was investigated using molecular dynamics simulation. The purpose of evaluating the stress distribution of CNTs is to characterize the loading transfer efficiency between the nano-reinforcement and surrounding polyimide matrix, which basically is an essential factor controlling the mechanical properties of nanocomposites. Three different interfacial adhesions between the CNTs and polyimide molecular were considered, that is, vdW interaction, CNTs with surface modification, and covalent bond. The stress distribution of the CNTs was calculated by using the Lutsko atomistic stress formulation[1,2] and by taking the derivative of the potential functions as well. Results revealed that when the CNTs surface was modified, the higher load transfer efficiency from the polyimide to the CNTs was observed resulting in the higher modulus of the nanocomposites. It is noted that, if no surface modification on CNTs, the load transfer efficiency which basically depends on the intensities of the vdW interaction is relatively low. As a result, the surface modification on CNTs is an effective manner to improve the load transfer efficiency as well as the modulus of nanocomposite, which should be suggested in the fabrication of CNTs nanocomposites.

Keywords

nanocomposites, stress distribution, carbon nanotubes, interfacial adhesion

Introduction

Since carbon nanotubes (CNTs) were discovered by Iijima[3] using transmission electron microscopy in 1991; the remarkable mechanical properties have made the CNTs become the most attractive reinforcement in polymeric composites.[4,5] According to the theory of rule of mixture, the mechanical properties of the nanocomposites can be enhanced properly when stiffer reinforcements are introduced in the matrix. However, some results[6] revealed that the CNTs-reinforced nanocomposites cannot fully produce the impressive mechanical properties as expected by the rule of mixture. Mokashi et al.[7] further indicated that if the load cannot be effectively transferred from the polymer matrix to the CNTs, the Young's modulus and tensile strength of the nanocomposites could be less than that of pure resin. Apparently, the mechanical performance of the nanocomposites is quite relied on the load-transfer efficiency from the surrounding matrix to the CNTs, and thus understanding the stress transfer of the CNT embedded within the nanocomposites is an essential subject in the nanocomposites.

In conventional composites, the load transfer efficiency as well as the interfacial shear strength (ISS) between the fiber and composites is determined based on fragmentation tests[8–10] and fiber pull-out tests.[10–12] Nevertheless, for the nanocomposites, due to the nano/submicron scale of the reinforcement, it is difficult to measure the ISS empirically.[13,14] Instead, the numerical approach based on the concept of fiber pull-out test was

Department of Mechanical Engineering, National Chiao Tung University, Taiwan.

Corresponding author:
Jia-Lin Tsai, Department of Mechanical Engineering, National Chiao Tung University, Hsinchu, 300, Taiwan
Email: jialin@mail.nctu.edu.tw

employed extensively to predict the ISS of nanocomposites.[15–19] Gou et al.[15] examined the ISS of CNTs/epoxy nanocomposites using molecular dynamics (MD) simulation revealing the ISS is around 75 MPa. Lordi and Yao[16] studied the binding energy and sliding frictional stresses between CNTs and various matrix polymers indicating that the polymers with hydroxy and phenyl side-groups can exhibit strong interfacial adhesion. In addition, it was found that the helical polymer conformation is an essential factor to enhance the ISS. Frankland et al.[17] depicted that with relatively low density of chemical bonds in the interface, there is an order of magnitude improvement in the shear strength of CNT/polymer interface and the corresponding critical length required for load transfer would be decreasing. The same tendency that the chemical bonding can increase the interfacial shear strength of nanocomposites was also observed by Chowdhury and Okabe.[18] Zheng et al.[19] examined the influences of sidewall modification of the CNTs with various functional groups on the interfacial bonding. Results showed that with low densities of functionalized carbon atoms, the interfacial bonding strength between the CNTs and polymer matrix can be drastically increased. Based on the continuum mechanics approach, Li and Chou[20] compared the load transfer in CNTs-reinforced nanocomposites with van der Waals (vdW) interactions and prefect bonding. It was indicated that for the nanocomposites with perfect interface, the CNTs sustain higher shear stress and normal stress than those with only vdW interaction.

In light of the forgoing investigations, it is suggested when a covalent bond between the CNTs and surrounding polymer is established, the ISS can be dramatically modified. Because most results were derived based on the fiber pullout simulation, only was the ISS between the CNTs and polymer presented. There is no constructive correlation between the ISS and the mechanical properties of the nanocomposites established. In fact, the mechanical behaviors of the nanocomposites, such as the tensile Young's modulus, are mainly dependent on the load-transfer efficiency from the surrounding matrix to the nano-reinforcement. In other words, the amount of stress carried by the CNTs would influence the mechanical responses of the nanocomposites. If the loading applied on the nanocomposites can be effectively transferred into the CNTs, the efficiency of the reinforcement embedded in the nanocomposites would be radically improved. There are many factors influencing the load transfer efficiency, such as the non-bonded atomistic interaction, surface modification of CNTs, and covalently chemical bonding between the CNTs and matrix. The main objective of this study is to characterize the load transfer efficiency of the CNTs within the nanocomposites subjected to axial loading. The effects of the atomistic interactions between the CNTs and the surrounding polyimide on the load transfer efficiency of CNTs would be systematically explored. Furthermore, the correlations between the tensile moduli of nanocomposites and the load transfer efficiency in terms of different interfacial adhesions were also discussed.

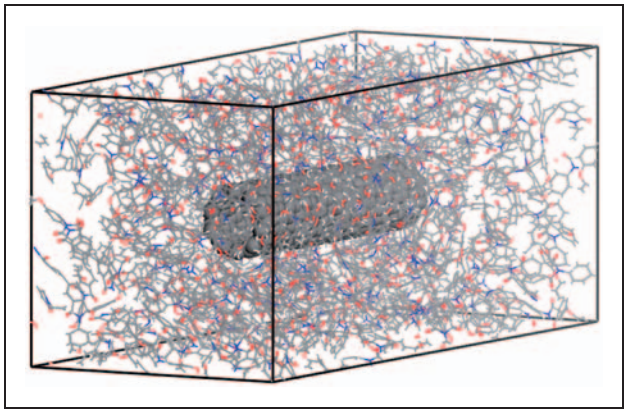

Figure 1. Molecular structure of carbon nanotubes (CNTs)/polyimide nanocomposites.

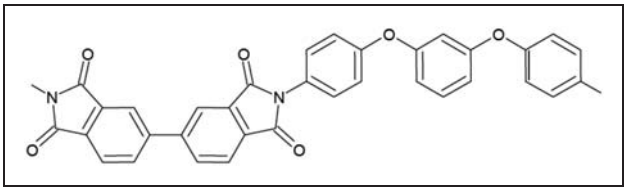

Figure 2. Schematic of polyimide monomer unit.

Construction of CNTS/polyimide nanocomposite model

In order to investigate the stress distribution of CNTs, the molecular structure of nanocomposites consisting of CNTs and polyimide polymer was constructed as shown in Figure 1. The (10, 0) zig-zag CNTs with diameter of 7.83 Å and length of 42.6 Å were considered a reinforcement embedded in the polyimide nanocomposites, while the polyimide containing 32 molecular chains was regarded as the polymer matrix. It is noted that each polyimide chain was generated by 10 monomer units. Figure 2 illustrates the polyimide monomer unit. To understand the influences of atomistic interactions on the load transfer efficiency as well as the modulus of the nanocomposites, three different interfacial adhesions between the CNTs and polyimide polymer were taken into account, that is, non-bonded vdW interaction, CNTs with surface modification, and covalent bond. It is noted that the vdW interaction was always taking place between the CNTs and polyimide polymer, even when the CNTs with surface modification and the covalent bond were considered in the simulation. For the CNTs surface modification, there are eight polyethylene polymer chains

(C_5H_{11}) adhered axial-symmetrically on the CNTs' surface as shown in Figure 3. The reason for such arrangement of the polyethylene chains is to easily explore the influence of surface modification on the stress distribution of the CNTs. With regard to the covalently bonded interaction, the polyethylene chains originally adhered on the CNTs' surface were further bonded to the polyimide molecular chains. The connection was accomplished by establishing the covalent bonds between the carbon atoms at the ends of polyethylene chains and the carbon atoms in the polyimide chains. As a result, the interatomistic relation between the CNTs and the surround polyimide matrix is not only vdW force but also the covalently bonded interaction.

Potential function

In the MD simulation, two kinds of interactions generally have been accounted for in modeling the interatomistic behaviors of the atoms,[21–22] that is, one is the bonded interaction, such as the covalent bonding, and the other is the non-bonded interaction, that is, vdW forces. The bonded interaction can be described using the potential energy that[23] consists of bond stretching, bond angle bending, torsion, and inversion as shown in Figure 4, and the explicit form of which is expressed as:

$$U_{\text{bond}} = \sum U_r + \sum U_\theta + \sum U_\phi + \sum U_\omega \quad (1)$$

where U_r is a bond stretching potential; U_θ is a bond angle bending potential; U_ϕ is a dihedral angle torsional potential; and U_ω is an inversion potential. For the CNTs, the detail expression of the bonded potentials can be found elsewhere,[24] while the non-bonded atomistic interaction between the carbon atoms was modeled using the Lennard-Jones (L-J) potential as:

$$U_{\text{vdW}} = 4u\left[\left(\frac{r_0}{r_{ij}}\right)^{12} - \left(\frac{r_0}{r_{ij}}\right)^{6}\right] \quad (2)$$

where r_{ij} is the distance between the non-bonded pair of atoms. For the hexagonal graphite, the parameters $u = 0.0556$ kcal/mole and $r_0 = 3.40$ Å suggested in the literature[25] were adopted in the modeling. Moreover, the cutoff distance for the vdW force was assigned to be 10 Å, which means that beyond this distance, there are no vdW interactions taking place.

For the polyimide polymer, the bond and non-bonded interactions among the molecular chains were modeled based on the Dreiding force field.[26] It is noted that in the Dreiding force field, the non-bonded interaction was also depicted by the L-J potential, the parameters of which between two different kinds of atoms were derived from the Lorentz Berthelot combining rule.[27] Moreover, the

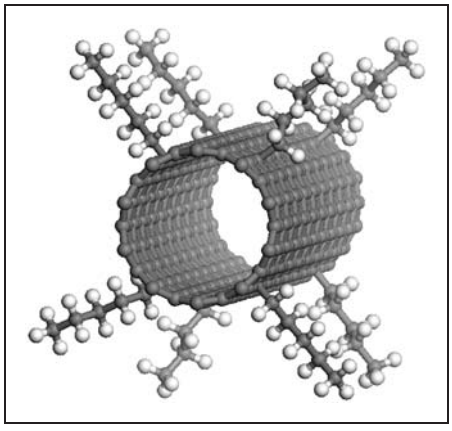

Figure 3. Carbon nanotubes (CNTs) with surface modification of polyethylene chains.

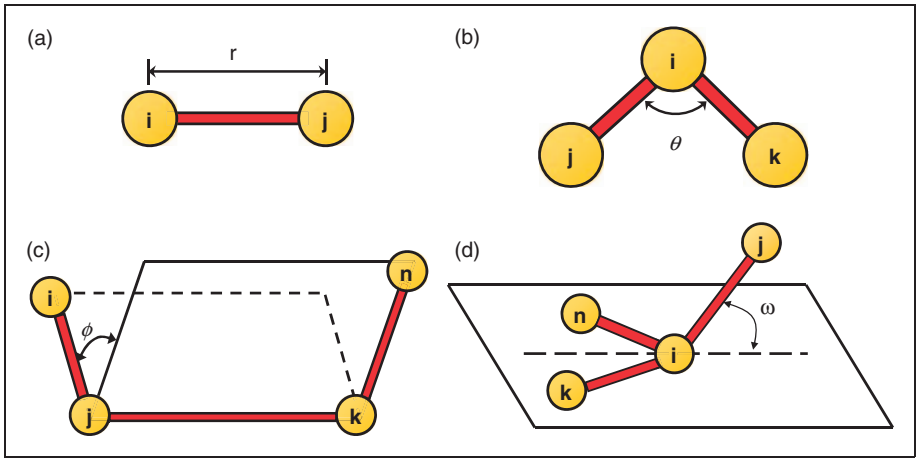

Figure 4. A schematic representation of the bonded potentials ((a) bond stretch, (b) valence angle potential, (c) dihedral potential, and (d) inversion potential).

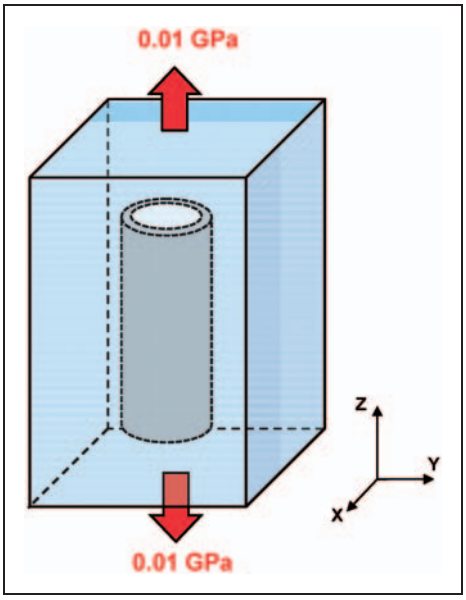

Figure 5. Carbon nanotubes (CNTs)/polyimide nanocomposites subjected to uniaxial loading.

atomistic interactions between CNTs and polyimide polymers were described using the L-J potential. In order to investigate the influence of vdW intensity on the load transfer efficiency, four different degrees of vdW interactions, that is, 0.01, 0.1, 1, and 5 times, between the CNTs and surrounding polyimide polymer were considered in the study. It should be noted that the resultant vdW force associated with 1 time of vdW interactions between the CNTs and polymer is around 0.88 nN in our simulation.

Molecular dynamic simulation of CNTs/polyimide nanocomposites

The equilibrated molecular structure of CNTs/polyimide nanocomposites with minimized energy was accomplished by sequentially performing the NVT and NPT ensembles in the MD simulation with time increment of 1 femtosecond (fs). It is noted that NVT ensemble stands for the number of atoms (N), volume (V), and temperature (T) being fixed during the simulation, and NPT ensemble represents that the number of atoms (N), pressure (P), and temperature (T) remain constant during the simulation. The purpose of the NVT ensemble conducted at 1000 K for 400 picosecond (ps) was to supply enough kinetic energy on the polyimide molecular so that homogeneous molecular structure within the simulation box can be achieved. In the NVT ensemble, the carbon atoms on CNTs were fixed at their original position throughout the whole simulation.[28] Subsequently, the NPT process was designated to 0 atm such that the simulation box with stress-free boundary condition can be achieved. Three sub-steps were introduced in the NPT process for the temperature reduction from 1000 to 0 K. In the first and second steps, the temperature was designated at 600 K and 300 K, respectively, and the simulation time in each step was 200 ps with time increment of 1 fs. In the third step, the modified NPT ensemble[29] with the characteristics of varying simulation box in shape and size was employed to obtain the molecular structures of nanocomposites with stress-free condition. It is noted that, during the modified NPT ensemble, the frozen atoms of CNTs in the nanocomposites were released and the corresponding temperature is allocated at 0 K. Subsequently, the uniaxial loading (0.01 GPa) was applied on the boundary of the simulation box in Z direction as shown in Figure 5. The corresponding equilibrated molecular structure subjected to uniaxial loading was obtained after the modified NPT ensemble was performed in the MD simulation with the time increment of 1 fs for 200 ps. In this study, the MD simulations were conducted using a DL-POLY package[30] which is existing software. However, for the simulation of the modified NPT ensemble as well as the calculation of the stress distribution on CNTs based on Lutsko stress formulation, we have to develop our own home-made subroutine.

Density distribution

The density distribution of polyimide polymer near the CNTs was first examined based on the atomistic morphology of the nanocomposites derived from the MD simulation. Figure 6 illustrates the cross-section of CNTs/polyimide nanocomposites, and the density distribution of polyimide along the radial direction was evaluated as:

$$\rho(r) = \frac{g_r}{V_r} \tag{3}$$

where $V_r = \pi((r + dr)^2 - r^2)L_0$ indicates the volume of a cylindrical shell near the CNTs with length equal to L_0, and g_r denotes the total atom mass within V_r. Figure 7 shows the density distribution of polyimide polymer in the radial direction in terms of different degrees of vdW interactions. It is observed that the polymer density is relatively high near the CNTs, and then declines to a typical value of 1.31 g/cc[31] as the location is little far away from the CNTs. Furthermore, when the intensity of vdW interaction is stronger, the polymer around the CNTs is denser. Apparently, the density distribution of the polyimide is noticeably influenced by the presence of the CNTs and the high-density polyimide near the CNTs may play an essential role in the load transfer efficiency of nanocomposites.

Stress calculation

Definition of atomic stress

In order to understand the load transfer in the nanocomposites, the stress distribution on the CNTs has to be appropriately evaluated. In this study, the Lutsko stress formulation[1,2]

$$\sigma^{\text{Lutsko}} = -\frac{1}{V^{\text{Lutsko}}}\left\{\sum_{\alpha=1}^{N} m^{\alpha}\mathbf{v}^{\alpha}\otimes\mathbf{v}^{\alpha} + \frac{1}{2}\sum_{\alpha=1}^{N}\sum_{\beta\neq\alpha}^{N}\mathbf{r}^{\alpha\beta}\otimes\mathbf{F}^{\alpha\beta}l^{\alpha\beta}\right\} \tag{4}$$

was employed to calculate the stress distribution on CNTs. In Equation (4), m^{α} and v^{α} represent the mass and velocity of atom α, respectively. ⊗ represents the tensor product of two vectors. $r^{\alpha\beta} = r^{\alpha} - r^{\beta}$ where r^{α} and r^{β} denote the positions of atom α and β, respectively. $F^{\alpha\beta}$ is the interatomic force between atoms α and β. V^{Lutsko} denotes the average volume and $l^{\alpha\beta}$ indicates the fraction of the length of the α – β bond lying inside the average volume. In general, Lutsko stress formulation provides the averaged value of the stress within the selected volume. In this analysis, a hollow cylinder with length of 10 Å and thickness of 3.4 Å as shown in Figure 8 was adopted as V^{Lutsko} to calculate the Lutsko stress along the CNTs

Validation of Lutsko stress formulation

The applicability of the Lutsko stress formulation to evaluate the stress distribution of CNTs was validated at first. A (10, 0) CNTs (with diameter of 7.83 Å and length of 42.6 Å) subjected to an axial deformation was employed for the demonstration. By applying a small

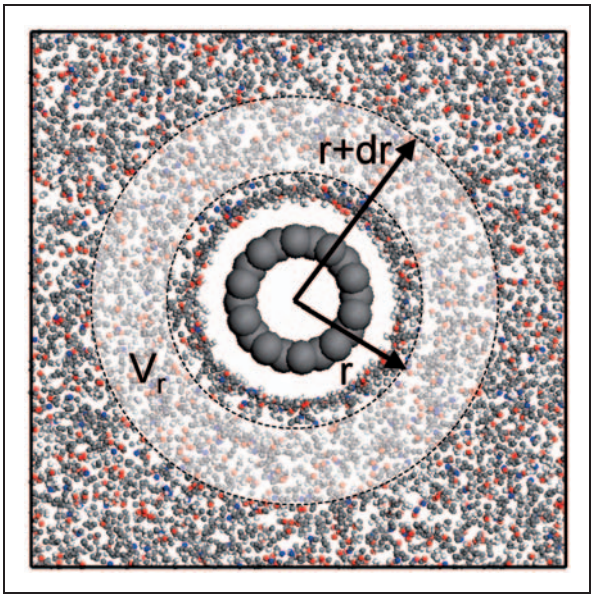

Figure 6. Selection of a cylindrical volume element for calculating polyimide density distribution.

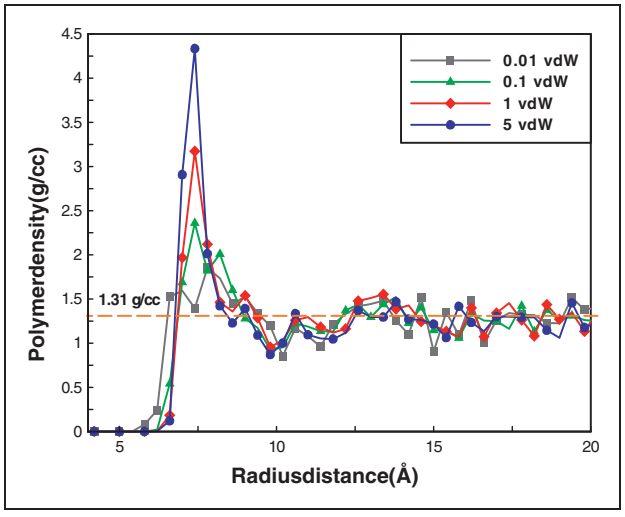

Figure 7. Density distribution of polyimide in the radial direction associated with four different intensities of vdW interactions.

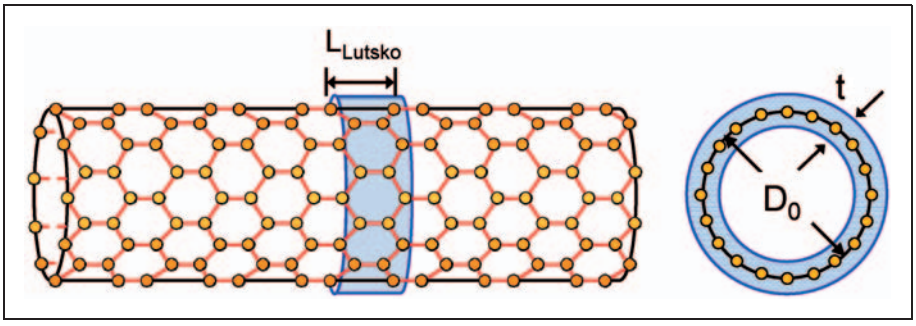

Figure 8. Schematic of Lutsko volume ($L_{\text{Ltusko}} = 10$ Å, $t = 3.4$ Å).

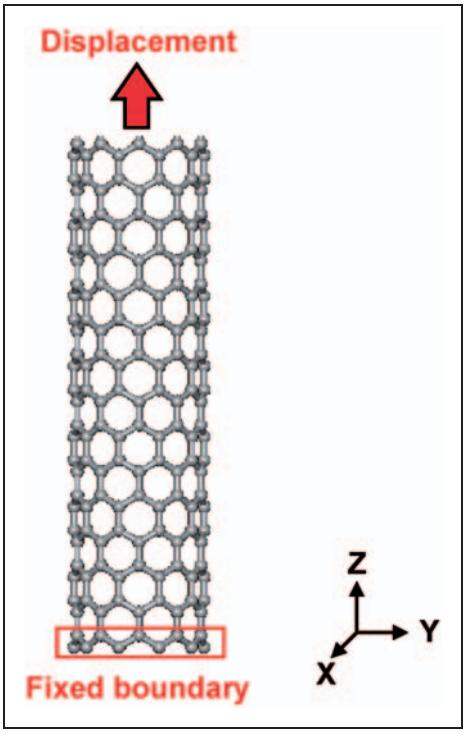

Figure 9. Axial deformation of carbon nanotubes (CNTs).

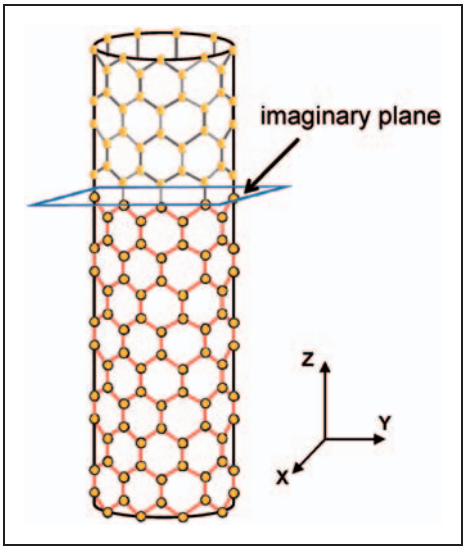

Figure 10. Imaginary plane assumed on the carbon nanotubes (CNTs).

axial displacement (0.0426 Å) at one end of the CNTs as shown in Figure 9, the deformed configuration of the CNTs was obtained directly from the energy minimization process. Due to the axial deformation, the corresponding normal stress generated on the CNTs should be evaluated properly through the Lutsko stress formulation, if it is applicable. In addition to the Lutsko stress formulation, the stress distribution of CNTs can also be calculated from the atomistic interactions between the carbon atoms associated with the bonded and non-bonded potentials. An imaginary plane crossing the cross section of CNTs was assumed and the possible atomistic interactions passing through the imaginary plane were then calculated in terms of the potential functions. It is noted that the simulation was conducted at 0 K, the kinetic energy was disregarded and only the potential energy was considered in the stress calculation. Figure 10 illustrates the imaginary plane on the CNTs. By taking the derivative of the potential function, the forces F_{int} infiltrating the imaginary plane was obtained, and then the axial stress along the CNTs was calculated as:

$$\sigma_{\text{int}} = \frac{F_{\text{int}}}{A} \tag{5}$$

where A is the cylindrical cross section of CNTs. The stress distributions of CNTs calculated based on the Lutsko stress formulation and the potential function were compared in Figure 11. It can be seen that the stress calculated based on the derivative of the potential function are quite uniform along the CNTs and the corresponding value is equal to the applied loading. However, for the Lutsko stress, although the value is remaining constant in the middle portion of CNTs, it begins to drop near the ends of the CNTs. This decreasing behavior is due to the fact that at the ends of CNTs, only part of atomistic interactions was included in the average volume V^{Lutsko} for the stress calculation. The Lutsko formulation basically is derived from the statistic mechanics considering the average stress within the volume V^{Lutsko}. However, the 'potential function' is a straightforward approach that considers the derivative of potential function as the forces F_{int} interacting on the atoms. Although the originality of the two methods is different, the calculated stresses should be close to each other as shown in Figure 11. In light of the forgoing discussion, it seems that both Lutsko stress formulation and the stress field based on the derivative of potential functions are capable of exhibiting the stress distribution of deformed CNTs. Thus, both approaches were employed to calculate the stress distribution of the CNTs embedded in the nanocomposites when the nanocomposites are subjected to the axial loading.

Stress distribution on CNTS in the nanocomposites

When the uniaxial loading (0.01 GPa) was applied on the boundary of the CNTs/polyimide nanocomposites as shown in Figure 5, the equilibrated molecular structure of nanocomposites was achieved by conducting the modified NPT ensemble[29] with time increment of 1 fs for 200 ps. In order to explore the influences of

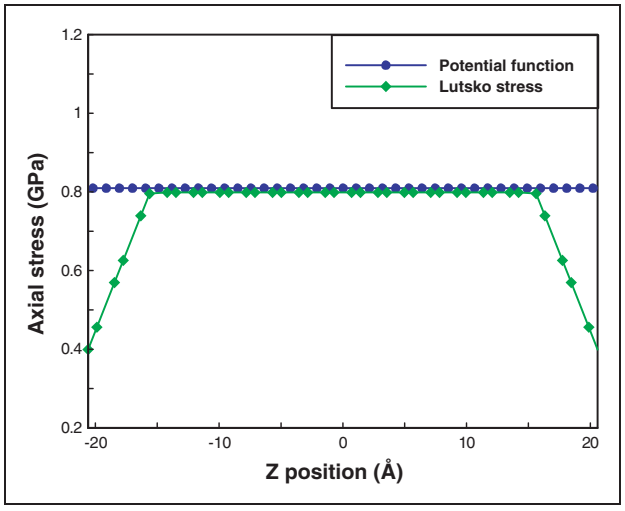

Figure 11. Calculation of axial stress distribution along the carbon nanotubes (CNTs).

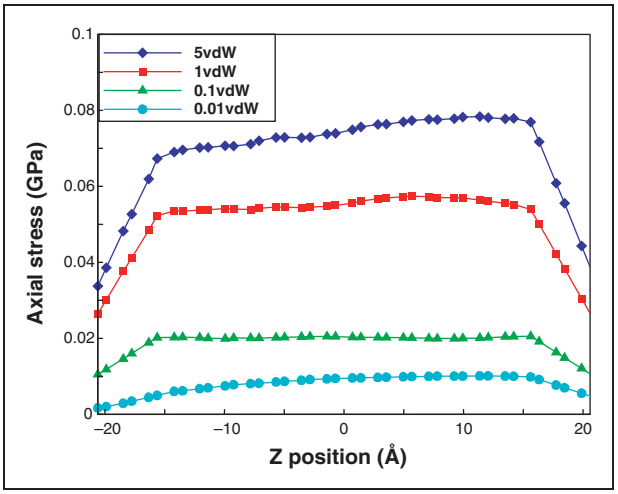

Figure 12. Axial stress distribution in the carbon nanotubes (CNTs) associated with four different degrees of vdW interactions (based on Lutsko stress formulation).

interfacial adhesions on the load transfer efficiency as well as the mechanical properties of nanocomposites, the stress distribution of the CNTs was calculated using the Lutsko stress formulation and the potential function. Figure 12 indicates the load transfer from the surrounding matrix to the CNTs associated with different degrees of vdW interactions. Apparently, when the vdW interaction is getting strong, the corresponding stress field on the CNTs is high accordingly, which imply that the load transfer from the polyimide to the CNTs is more efficient. In addition, it is observed that the axial stress is distributed almost uniformly along the CNTs. This phenomenon suggests that the load is transferred to the CNTs mostly through the CNTs both ends

Table 1. Comparison of longitudinal moduli of carbon nanotubes (CNTs)/polyimide nanocomposites with different degrees of van der Waals (vdW) interactions

Degrees of vdW interaction	Longitudinal modulus (GPa)
0.01 vdW	4.19
0.1 vdW	4.21
1 vdW	4.3
5 vdW	4.9

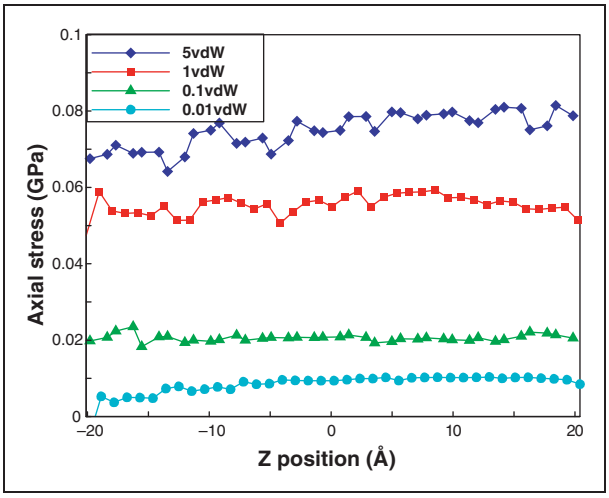

Figure 13. Axial stress distribution in the carbon nanotubes (CNTs) associated with four different degrees of vdW interactions (based on potential function).

rather than by means of the CNTs wall surface. It is noted that the stress distribution of CNTs calculated from the current molecular model is different from that obtained from Cox model,[32] although both set up are the same. In Cox model, the CNTs are assumed to be perfectly bonded to linear elastic matrix and the stress can be transferred to the CNTs mainly by the shear force acting on the wall surface. Therefore, the stress in the CNTs would increase from both ends and then reach a peak value in the middle section. On the contrary, in the molecular model, because the wall of CNTs is quite smooth and the vdW interaction through the wall surface is not effective, the load transfer may not be as efficient as that predicted in Cox model. The moduli of the CNTs nanocomposites associated with different intensities of vdW are summarized in Table 1. It can be seen that the moduli of the nanocomposites are also improved by the increase of vdW interactions. It is noted that since the stress fields shown in Figure 12 were calculated based on Lutsko stress formulation, there is a perceptible stress drop near the ends of the CNTs. On the other hand, when we evaluated the stress distributions using the potential function approach, it can be seen in Figure 13 that there is no significant stress drop

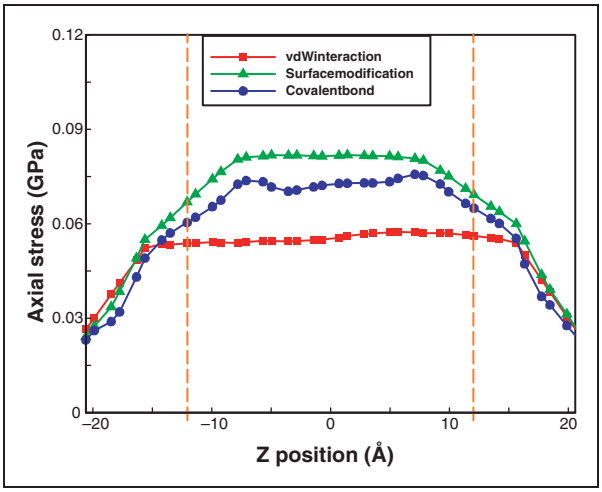

Figure 14. Comparison of axial stress distribution of carbon nanotubes (CNTs) with three different interfacial adhesions based on Lutsko stress formulation (vdW interaction, surface modification, and covalent bond).

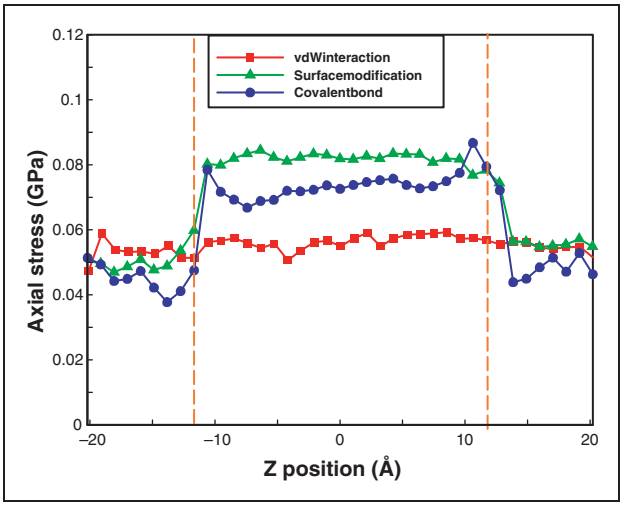

Figure 15. Comparison of axial stress distribution of carbon nanotubes (CNTs) with three different interfacial adhesions based on potential function (van der Waals [vdW] interaction, surface modification, and covalent bond).

Table 2. Comparison of longitudinal moduli of carbon nanotubes (CNTs)/polyimide nanocomposites with different interfacial adhesions

Interfacial adhesions	Longitudinal modulus (GPa)
van der Waals (vdW) interaction	4.3
Surface modification	4.52
Covalent bond	4.41

near the ends. The almost uniform stress distribution again validated the fact that the load was transferred into the CNTs mostly through the CNTs ends. In addition to the vdW interactions, the influences of the surface modification and the covalent bond on the mechanical responses of nanocomposites were also examined. Figure 14 demonstrates the stress distribution of CNTs associated with three different interfacial adhesions. It is noted that the stress curves shown in Figure 14 were calculated based on the Lutsko stress formulation. The corresponding moduli of the nanocomposites are also presented in Table 2. It is illustrated that the CNTs with surface modification exhibit both higher load transfer efficiency and higher moduli of nanocomposites as compared to the other two cases. This improvement could be due to the entangle effect between the polyethylene surfactant and the polyimide matrix. When the nanocomposites are subjected to loading, because of the mismatch of the constituent materials, there is a relative deformation taking place in the interface. If the interfacial bonding is weak, the relative displacement is large and the load transfer efficiency is relatively less. On the contrary, if the interfacial bonding becomes strong, the relative displacement would be less and the load transfer efficiency would be increased. The purpose of the polyethylene surfactant is to improve 'friction' between the CNTs and polyimide matrix, and meanwhile to lessen the relative displacement so that the load can be effectively transferred into the CNTs. The effect of the polyethylene surfactant can be clearly demonstrated from Figure 15 in which the stress curves were calculated based on the potential approach. It can be seen that around the positions where the surfactants were attached on CNTs (indicated by the dash line), the axial stresses rise dramatically. This phenomenon reveals that the loads can be efficiently transferred into the CNTs through the CNTs surfactant. In addition, it was found that the covalent bonding provides almost the same enhancement as the surface modification. In other words, the function of covalent bond is not completely exhibited in the current simulation. There are several factors causing the results, that is, the size of the simulation box, the connection of the covalent bond, and the selection of surfactant. The details regarding the influence of the covalent bonding on the mechanical responses of nanocomposites will be explored in the near future.

Conclusions

The load transfer efficiency of CNTs/polyimide nanocomposites in terms of different interfacial adhesions was investigated by accounting for the atomistic interactions between the CNTs and the polymeric matrix, which was rarely explored in literature. The stress distribution of

the CNTs embedded in polyimide nanocomposites was calculated through Lutsko stress formulation and the derivative of the potential function, from which the load transfer efficiency was characterized. It was found that taking the derivative of the potential function is an appropriate manner to calculate the 'local' stress distribution of CNTs, since it can prevent the perceptible stress drop near the ends of CNTs. Moreover, it is revealed when the CNTs surfaces were modified, the load transfer efficiency of nanocomposites could be appreciably enhanced by the surfactants. As a result, the surface modification needs to be employed in the fabrication process of CNTs to effectively improve the mechanical properties of nanocomposites. In addition, the load transfer efficiency as well as the moduli of the nanocomposites could also be modified by adjusting the intensities of the vdW interactions. However, the vdW force was transferred into the CNTs mostly through the CNTs ends rather than by CNTs wall surface, which is unusual in the conventional fiber composites. With regard to the formation of covalent bond, due to the limited size of the molecular structures, the effect is almost the same as that of the surface modification. A further study is required to understand the influence of the covalent bonds on the mechanical properties of nanocomposites.

This research received no specific grant from any funding agency in the public, commercial, or not-for-profit sectors.

References

1. Lutsko JF. Stress and elastic constants in anisotropic solids: Molecular dynamics techniques. *J Appl Phys* 1988; 64(3): 1152–1154.
2. Cormier J, Rickaman JM and Delph TJ. Stress calculation in atomistic simulations perfect and imperfect solids. *J Appl Phys*. 2001; 89(1): 99–104.
3. Iijima S. Helical microtubules of graphitic carbon. *Nature* 1991; 354(6348): 56–58.
4. Lau KT, Gu C and Hui D. A critical review on nanotube and nanotube/nanoclay related polymer composite materials. *Compos Part B-Eng* 2006; 37(6): 425–436.
5. Thostenson ET, Ren Z and Chou TW. Advances in the science and technology of carbon nanotubes and their composites: a review. *Compos Sci Technol* 2001; 61(13): 1899–1912.
6. Shim BS, Zhu J, Jan E, Critchley K, Ho S, Podsiadlo P, et al. Multiparameter structural optimization of single-walled carbon nanotube composites: toward record strength, stiffness, and toughness. *ACS Nano* 2009; 3(7): 1711–1722.
7. Mokashi VV, Qian D and Liu Y. A study on the tensile response and fracture in carbon nanotube-based composites using molecular mechanics. *Compos Sci Technol* 2007; 67(3-4): 530–540.
8. Yavin B, Gallis HE, Scherf J, Eitan A and Wagner HD. Continuous monitoring of the fragmentation phenomenon in single fiber composite materials. *Polym Composite* 1991; 12(6): 436–446.
9. Andersons J, Joffe R, Hojo M and Ochiai S. Fibre fragment distribution in a single-fibre composite tension test. *Compos Part B-Eng* 2001; 32(4): 323–332.
10. Valadez-Gonzalez A, Cervantes-Uc JM, Olayo R and Herrera-Franco PJ. Effect of fiber surface treatment on the fiber-matrix bond strength of natural fiber reinforced composites. *Compos Part B-Eng* 1999; 30(3): 309–320.
11. Moon CK. The effect of interfacial microstructure on the interfacial strength of glass fiber/polypropylene resin composites. *J Appl Polym Sci* 1994; 54(1): 73–82.
12. Piggott MR and Dai SR. Fiber pull out experiments with thermoplastics. *Polym Eng Sci* 1991; 31(17): 1246–1249.
13. Al-Haik M, Hussaini MY and Garmestani H. Adhesion energy in carbon nanotube-polyethylene composite: Effect of chirality. *J Appl Phys* 2005; 97(7): 074306.
14. Namilae S and Chandra N. Multiscale model to study the effect of interfaces in carbon nanotube-based composites. J Eng Mater-T ASME. 2005; 127(2): 222–232.
15. Gou J, Minaie B, Wang B, Liang Z and Zhang C. Computational and experimental study of interfacial bonding of single-walled nanotube reinforced composites. *Comp Mater Sci* 2004; 31(3–4): 225–236.
16. Lordi V and Yao N. Molecular mechanics of binding in carbon-nanotube polymer composites. *J Mater Res* 2000; 15(12): 2770–2779.
17. Frankland SJV, Caglar A, Brenner DW and Griebel M. Molecular simulation of the influence of chemical cross-links on the shear strength of carbon nanotube-polymer interfaces. *J Phys Chem B* 2002; 106(12): 3046–3048.
18. Chowdhury SC and Okabe T. Computer simulation of carbon nanotube pull-out from polymer by the molecular dynamics method. *Compos Part A-Appl S* 2007; 38(3): 747–754.
19. Zheng Q, Xia D, Xue Q, Yan K, Gao X and Li Q. Computational analysis of effect of modification on the interfacial characteristics of a carbon nanotube-polyethylene composite system. *Appl Surf Sci* 2009; 255(6): 3534–3543.
20. Li C and Chou TW. Multiscale modeling of carbon nanotube reinforced polymer composites. *J Nanosci Nanotechno* 2003; 3(5): 423–430.
21. Han Y and Elliott J. Molecular dynamics simulations of the elastic properties of polymer/carbon nanotube composites. *Comp Mater Sci* 2007; 39(2): 315–323.
22. Frankland SJV, Harik VM, Odegard GM, Brenner DW and Gates TS. The stress-strain behavior of polymer–nanotube composites from molecular dynamics simulation. *Compos Sci Technol* 2003; 63(11): 1655–1661.
23. Rappe AK and Casewit CJ. *Molecular mechanics across chemistry*. Sausalito, CA: University Science Books, 1997.
24. Tsai JL, Tzeng SH and Chiu YT. Characterizing elastic properties of carbon nanotubes/polyimide nanocomposites using multi-scale simulation. *Compos Part B-Eng* 2010; 41(1): 106–115.
25. Battezzatti L, Pisani C and Ricca F. Equilibrium conformation and surface motion of hydrocarbon molecules physisorbed on graphite. *J Chem Soc* 1975; 71: 1629–1639.

26. Mayo SL, Olafson BD and Goddard III WA. DREIDING: a generic force field for molecular simulations. *J Phys Chem* 1990; 94(26): 8897–8909.
27. Allen MP and Tildesley DJ. *Computer simulation of liquids*. Oxford: Oxford University Press, 1989.
28. Adnan A, Sun CT and Mahfuz H. A molecular dynamics simulation study to investigate the effect of filler size on elastic properties of polymer nanocomposites. *Compos Sci Technol* 2007; 67(3–4): 348–356.
29. Melchionna S, Ciccotti G and Holian BL. Hoover NPT dynamics for systems varying in shape and size. *Mol Phys* 1993; 78(3): 533–544.
30. Smith W, Forester TR. DLPOLY-2.13 manual, 2001.
31. Ashby MF and Jones DR. *Engineering materials 1: An introduction to their properties and applications*. Oxford: Butterworth-Heinemann, 1996.
32. Cox HL. The elasticity and strength of paper and other fibrous materials. *Br J Appl Phys* 1952; 3: 72–79.